A Columnar Phase of Dendritic Lipid−Based Cationic Liposome−DNA Complexes for Gene Delivery: Hexagonally Ordered Cylindrical Micelles Embedded in a DNA Honeycomb Lattice

Kai K. Ewert, Heather M. Evans,[†] Alexandra Zidovska, Nathan F. Bouxsein,
Ayesha Ahmad,[§] and Cyrus R. Safinya*

*Contribution from the Department of Materials, Department of Physics, and Molecular,
Cellular and Developmental Biology Department, University of California,
Santa Barbara, California 93106*

Received August 26, 2005; E-mail: safinya@mrl.ucsb.edu

Abstract: Gene therapy holds great promise as a future approach to fighting disease and is explored in worldwide clinical trials. Cationic liposome (CL)−DNA complexes are a prevalent nonviral delivery vector, but their efficiency requires improvement and the understanding of their mechanism of action is incomplete. As part of our effort to investigate the structure-transfection efficiency relationships of self-assembled CL−DNA vectors, we have synthesized a new, highly charged (16+) multivalent cationic lipid, MVLBG2, with a dendritic headgroup. Our synthetic scheme allows facile variation of the headgroup charge and the spacer connecting hydrophobic and headgroup moieties as well as gram-scale synthesis. Complexes of DNA with mixtures of MVLBG2 and neutral 1,2-dioleoyl-*sn*-glycerophosphatidylcholine (DOPC) exhibit the well-known lamellar phase at 90 mol % DOPC. Starting at 20 mol % dendritic lipid, however, two novel nonlamellar phases are observed by synchrotron X-ray diffraction. The structure of one of these phases, present in a narrow range of composition around 25 mol % MVLBG2, has been solved. In this novel dual lattice structure, termed H_I^C, hexagonally arranged tubular lipid micelles are surrounded by DNA rods forming a three-dimensionally continuous substructure with honeycomb symmetry. Complexes in the H_I^C phase efficiently transfect mouse and human cells in culture. Their transfection efficiency, as well as that of the lamellar complexes containing only 10 mol % dendritic lipid, reaches and surpasses that of commercially available, optimized DOTAP-based complexes. In particular, complexes containing MVLBG2 are significantly more transfectant over the entire composition range in mouse embryonic fibroblasts, a cell line empirically known to be hard to transfect.

Introduction

Somatic gene therapy, i.e., the use of DNA as a therapeutic agent, holds great promise for future medical applications. Indeed, numerous clinical trials in this field are currently ongoing.[1,2] Cancers, inherited diseases, cardiovascular diseases, and many others are targets for this novel medical approach.[3,4] In fact, the therapeutic prospects of nucleic acid delivery are expanding constantly[5] due to recent discoveries such as that of RNA interference (RNAi), which enables, in principle, selective gene silencing.[6−9] Thus, substantial research efforts are directed toward developing and fundamentally understanding DNA carriers (vectors). Engineered viruses are very efficient vectors,[10,11] but general concerns about their safety have recently been intensified by a few severe setbacks.[12] This has further increased the interest in nonviral or synthetic vectors,[13−15] in which the negatively charged DNA is complexed with cationic

† Current address: Max Planck Institute for Dynamics and Self-Organization, Bunsenstrasse 10, D-37073 Göttingen, Germany.

§ Current address: Imperial College Genetic Therapies Centre, Department of Chemistry, Flowers Building, Armstrong Road, Imperial College London, London, SW7 2AZ, U.K.

(1) Extensive and current information on clinical trials in the field of gene therapy can be found on the Internet at http://www.wiley.co.uk/genetherapy/clinical/. See Ewert, K.; Ahmad, A.; Evans, H. M.; Safinya, C. R. *Expert Opin. Biol. Ther.* **2005**, *5*, 33−53 for a compilation of open trials in nonviral gene therapy as of July 2004.
(2) Griesenbach, U.; Geddes, D. M.; Alton, E. W. F. W. In *Nonviral Vectors for Gene Therapy*; Huang, L., Hung, M.-C., Wagner, E., Eds.; Academic Press: San Diego, 1999; pp 337−356.
(3) Felgner, P. L.; Rhodes, G. *Nature* **1991**, *349*, 351−352.
(4) Smyth-Templeton, N., Lasic, D. D., Eds. *Gene Therapy. Therapeutic Mechanisms and Strategies*; Marcel Dekker Inc.: New York, 2000.

(5) Mahato, R. I., Kim, S. W., Eds. *Pharmaceutical Perspectives of Nucleic Acid-Based Therapeutics*; Taylor and Francis: London and New York, 2002.
(6) McManus, M. T.; Sharp, P. A. *Nat. Rev. Genet.* **2002**, *3*, 737−747.
(7) Caplen, N. J. *Gene Ther.* **2004**, *11*, 1241−1248.
(8) Milner, J. *Expert Opin. Biol. Ther.* **2003**, *3*, 459−467.
(9) Caplen, N. J. *Expert Opin. Biol. Ther.* **2003**, *3*, 575−586.
(10) Smith, A. E. *Annu. Rev. Microbiol.* **1995**, *49*, 807−838.
(11) Kay, M. A.; Glorioso, J. C.; Naldini, L. *Nature Med.* **2001**, *7*, 33−40.
(12) (a) Marshall, E. *Science* **2000**, *288*, 951−957. (b) Marshall, E. *Science* **2002**, *298*, 510−511.
(13) Huang, L., Hung, M.-C., Wagner, E., Eds. *Non-Viral Vectors for Gene Therapy*, 2nd ed., Part I; Advances in Genetics, Vol. 53; Elsevier: San Diego, 2005.
(14) Huang, L., Hung, M.-C., Wagner, E., Eds.; *Nonviral Vectors for Gene Therapy*; Academic Press: San Diego, 1999.
(15) Felgner, P. L., Heller, M. J., Lehn, P., Behr, J.-P., Szoka, F. C., Eds.; *Artificial Self-Assembling Systems for Gene Delivery*; American Chemical Society: Washington, DC, 1996.

liposomes (CLs)[16–19] or cationic polyelectrolytes.[20–22] Synthetic vectors have several advantages over viral methods, such as facile and variable preparation, absence of immunogenic protein components, and unlimited length of the transported DNA. A large number of cationic and other lipids for use in gene delivery have been synthesized. The earlier part of these efforts has been reviewed in detail,[23–25] and several more recent reviews with a smaller scope have also appeared.[26–28] Several lipid vectors have been commercialized, and many are able to efficiently transfect cultured mammalian cells. For CL−DNA complexes to become widely useful for gene therapeutic purposes, however, their efficiency needs to be improved.[29]

The improvement of CL−DNA vectors requires a better understanding of their mechanism of transfection, and the chemical and physical parameters of CL−DNA complexes influencing it. Thus, a large amount of work has been performed in order to understand the formation and structure of CL−DNA complexes, and to establish correlations between the structures and physicochemical characteristics of the complexes and their transfection efficiency and mechanism of action.[30,31] Thus far, two equilibrium structures of CL−DNA complexes have been found: the inverted hexagonal (H_{II}^C)[32] and the more abundant lamellar (L_α^C)[33,34] liquid crystal phase. These are schematically shown in Figure 1. In addition, kinetically trapped structures have been observed, e.g. by electron microscopy.[35] The transfection mechanisms of the two phases vary greatly as a consequence of their structures, but hexagonal and optimized lamellar complexes transfect equally well.[36–38] In addition to the composition and rigidity of the membrane,[32] the molecular
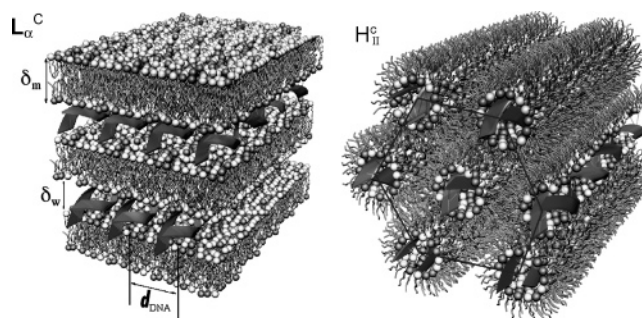

Figure 1. Schematic depictions of the previously known equilibrium phases of CL−DNA complexes, showing the local structure of their interior on the nanometer scale. Neutral and cationic lipids are depicted as having white and gray headgroups, respectively. The lamellar phase, L_α^C, consisting of alternating lipid bilayers and DNA monolayers with an interlayer spacing of d = $\delta_w + \delta_m$ is depicted on the left. The inverted hexagonal phase H_{II}^C, which is comprised of DNA rods coated with a lipid monolayer and arranged on a hexagonal lattice, is shown on the right. Adapted with permission from ref 32.

shape and corresponding preferred curvature of a lipid determines the structure of its DNA complexes. This is evident by the tendency of DOPE to promote the H_{II}^C phase, due to its cone-shaped molecular structure. Likewise, it seemed feasible to induce a complex structure with positive lipid curvature by using lipids with large headgroups (corresponding to an inverted cone molecular shape). However, lipids with 3−5 cationic charges in the headgroup still form L_α^C−DNA complexes,[39–41] even though some of these lipids (without DNA) have been shown to form spherical and wormlike micelles in solution.[41] To further increase the headgroup charge and size and, thus, possibly induce the formation of complexes containing such micellar structures, we have synthesized a new lipid with a highly charged, dendritic headgroup.

Dendrimers are monodisperse, highly branched synthetic molecules, which are typically assembled by adding generations of AB₂ monomers to a core molecule.[42–45] Dendrimers bearing amino groups that can be protonated, such as poly(amidoamine) (PAMAM) and poly(propylenimine) (PPI) dendrimers, have been used successfully for gene delivery,[46–50] and the structure of their DNA complexes has been investigated.[51] Conjugates of dendritic molecules to PEG have also been used for gene delivery.[52]

(16) Felgner, P. L.; Gader, T. R.; Holm, M.; Roman, R.; Chan, H. W.; Wenz, M.; Northrop, J. P.; Ringold, G. M.; Danielsen, M. *Proc. Natl. Acad. Sci. U.S.A.* **1987**, *84*, 7413−7417.
(17) Wheeler, C. J.; Felgner, P. L.; Tsai, Y. J.; Marshall, J.; Sukhu, L.; Doh, S. G.; Hartikka, J.; Nietupski, J.; Manthorpe, M.; Nichols, M.; Plewe, M.; Liang, X. Norman, J.; Smith, A.; Cheng, S. H. *Proc. Natl. Acad. Sci. U.S.A.* **1996**, *93*, 11454−11459.
(18) Byk, G.; Dubertret, C.; Escriou, V.; Frederic, M.; Jaslin, G.; Rangara, R.; Pitard, B.; Crouzet, J.; Wils, P.; Schartz, B.; Scherman, D. *J. Med. Chem.* **1998**, *41*, 224−235.
(19) Remy, J.-S.; Sirlin, C.; Vierling, P.; Behr, J.-P. *Bioconjugate Chem.* **1994**, *5*, 647−654.
(20) Boussif, O.; Lezoualc'h, F.; Zanta, M. A.; Mergny, M. D.; Scherman, D.; Demeniex, B.; Behr, J.-P. *Proc. Natl. Acad. Sci. U.S.A.* **1995**, *92*, 7297−7301.
(21) Haensler, J.; Szoka, F. C. *Bioconjugate Chem.* **1993**, *4*, 372−379.
(22) Tang, M. X.; Redemann, C. T.; Szoka, F. C. *Bioconjugate Chem.* **1996**, *7*, 703−714.
(23) Miller, A. D. *Angew. Chem., Int. Ed.* **1998**, *37*, 1769−1785.
(24) Zabner, J. *Adv. Drug Delivery Rev.* **1997**, *27*, 17−28.
(25) Behr, J.-P. *Bioconjugate Chem.* **1994**, *5*, 382−389.
(26) Byk, G.; Scherman, D. *Drug Dev. Res.* **2000**, *50*, 566−572.
(27) Chesnoy, S.; Huang, L. *Annu. Rev. Biophys. Biomol. Struct.* **2000**, *29*, 27−47.
(28) de Lima, M. C. P.; Simões, S.; Pires, P.; Faneca, H.; Düzgünes, N. *Adv. Drug Delivery Rev.* **2001**, *47*, 277−294.
(29) Miller, A. D. *Curr. Med. Chem.* **2003**, *10*, 1195−1211.
(30) Koltover, I.; Safinya, C. R. In *Nonviral Vectors for Gene Therapy*; Huang, L., Hung, M.-C., Wagner, E., Eds.; Academic Press: San Diego, 1999; pp 91−117.
(31) Safinya, C. R.; Lin, A. J.; Slack, N. L.; Koltover, I. In *Pharmaceutical Perspectives of Nucleic Acid-Based Therapeutics*; Mahato, R. I., Kim, S. W., Eds.; Taylor and Francis: London and New York, 2002; pp 190−210.
(32) Koltover, I.; Salditt, T.; Rädler, J. O.; Safinya, C. R. *Science* **1998**, *281*, 78−81.
(33) Rädler, J. O.; Koltover, I.; Salditt, T.; Safinya, C. R. *Science* **1997**, *275*, 810−814.
(34) Koltover, I.; Salditt, T.; Safinya, C. R. *Biophys. J.* **1999**, *77*, 915−924.
(35) Smyth Templeton, N.; Lasic, D. D.; Frederik, P. M.; Strey, H. H.; Roberts, D. D.; Pavlakis, G. N. *Nat. Biotechnol.* **1997**, *15*, 647−652.
(36) Lin, A. J.; Slack, N. L.; Ahmad, A.; Koltover, I.; George, C. X.; Samuel, C. E.; Safinya, C. R. *J. Drug Targeting* **2000**, *8*, 13−27.
(37) Ewert, K.; Slack, N. L.; Ahmad, A.; Evans, H. M.; Lin, A. J.; Samuel, C. E.; Safinya, C. R. *Curr. Med. Chem.* **2004**, *11*, 133−149.
(38) Ewert, K.; Ahmad, A.; Evans, H. M.; Safinya, C. R. *Expert Opin. Biol. Ther.* **2005**, *5*, 33−53.

(39) Ewert, K.; Ahmad, A.; Evans, H. M.; Schmidt, H.-W.; Safinya, C. R. *J. Med. Chem.* **2002**, *45*, 5023−5029.
(40) Ahmad, A.; Evans, H. M.; Ewert, K.; George, C. X.; Samuel, C. E.; Safinya, C. R. *J. Gene Med.* **2005**, *7*, 739−748.
(41) Boukhnikachvili, T.; Aguerre-Chariol, O.; Airiau, M.; Lesieur, S.; Ollivon, M.; Vacus, J. *FEBS Lett.* **1997**, *409*, 188−194.
(42) Bosman, A. W.; Janssen, H. M.; Meijer, E. W. *Chem. Rev.* **1999**, *99*, 1665−1688.
(43) Fischer, M.; Vögtle, F. *Angew. Chem., Int. Ed.* **1999**, *38*, 884−905.
(44) Frechet, J. M. J.; Tomalia, D. A., Eds. *Dendrimers and Other Dendritic Polymers*; Wiley: Chichester, 2001.
(45) Tomalia, D. A. *Sci. Am.* **1995**, *272*, 62−66.
(46) Tang, M. X.; Redemann, C. T.; Szoka, F. C. *Bioconjugate Chem.* **1996**, *7*, 703−714.
(47) Kukowaska-Latallo, J. F.; Bielinska, A. U.; Johnson, J.; Spindler, R.; Tomalia, D. A.; Baker, J. R. Jr. *Proc. Natl. Acad. Sci. U.S.A.* **1996**, *93*, 4897−4902.
(48) Kukowska-Latallo, J. F.; Raczka, E.; Quintana, A.; Chen, C. L.; Rymaszewski, M.; Baker, J. R., Jr. *Human Gene Ther.* **2000**, *11*, 1385−1395.
(49) Rudolph, C.; Lausier, J.; Naundorf, S.; Müller, R. H.; Rosenecker J. *J. Gene Med.* **2000**, *2*, 269−278.
(50) Ohsaki, M.; Okuda, T.; Wada, A.; Hirayama, T.; Niidome, T.; Aoyagi, H. *Bioconjugate Chem.* **2002**, *13*, 510−517.
(51) Evans, H. M.; Ahmad, A.; Ewert, K.; Pfohl, T.; Martin-Herranz, A.; Bruinsma, R. F.; Safinya, C. R. *Phys. Rev. Lett.* **2003**, *91*, 075501-1−075501-4.
(52) Kim, T. I.; Seo, H. J.; Choi, J. S.; Jang, H. S.; Baek, J. U.; Kim, K.; Park, J. S. *Biomacromolecules* **2004**, *5*, 2487−2492.
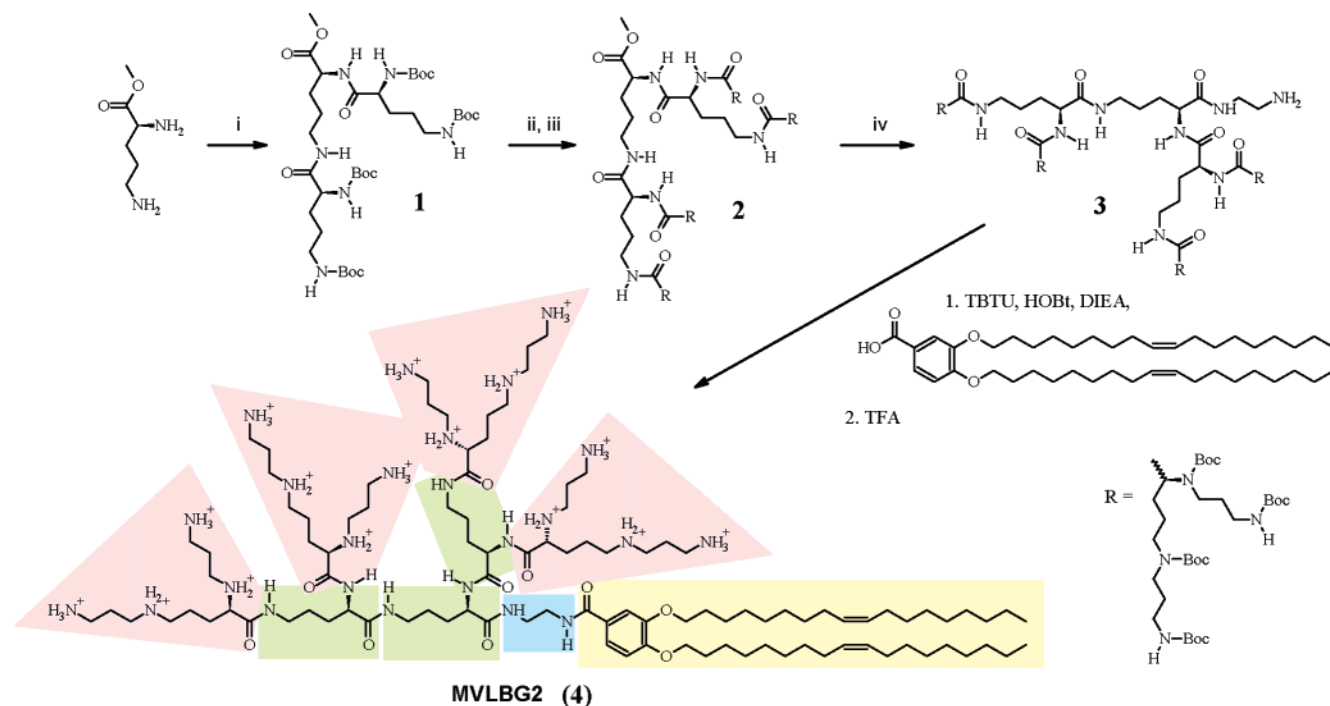
Figure 2. Synthesis of the dendritic lipid MVLBG2, starting from ornithine methyl ester. The hydrophobic DOB moiety, ethylenediamine spacer, ornithine headgroup core, and carboxyspermine endgroups are underlaid in yellow, blue, green, and red, respectively. Reaction conditions: i: Boc-L-ornithine(Boc), TBTU, HOBt, DIEA; ii: TFA; iii: R-COOH (**7**), TBTU, HOBt, DIEA; iv: excess ethylenediamine (20×) in MeOH. HOBt: 1-hydroxybenzotriazole hydrate; DIEA: *N,N*-diisopropylethylamine; TBTU: *O*-benzotriazol-1-yl-*N,N,N′,N′*-tetramethyluronium tetrafluoroborate; TFA: trifluoroacetic acid.

In this paper, we report the synthesis of a new multivalent cationic lipid, MVLBG2, with a dendritic headgroup. This headgroup has a core based on ornithine that is terminated by carboxyspermine moieties. The headgroup carries 16 positive charges at complete protonation, expanding the range of membrane charge density accessible by our experiments and approaching the realm of lipid−polymer and lipid−dendrimer hybrid materials, which have been reported occasionally.[53−57] In addition, this lipid can be viewed as an extension of the concept of multivalent lipids,[18,58,59] since few lipids with more than five charges per headgroup have been reported. Our synthetic scheme allows for gram-scale synthesis and facile variation of headgroup charge and the spacer connecting hydrophobic and headgroup moieties. We have prepared DNA complexes from mixtures of MVLBG2 with DOPC to investigate their structures using X-ray diffraction and measure their transfection efficiency with a luciferase reporter gene assay. X-ray diffraction shows that the complexes form the L_α^C phase[33] at low contents of dendritic lipid in the membrane. For higher contents of the highly charged MVLBG2, two nonlamellar phases are observed. The structure of one of these, present in a narrow range of composition around 25 mol % MVLBG2, has been solved. This phase, termed H_I^C and consisting of a hexagonal array of tubular micelles, constitutes a previously unknown, third phase of CL−DNA complexes. DNA rods are intercalated in the interstices to form a three-dimensionally contiguous substructure with honeycomb symmetry, as opposed to the isolated DNA rods and sheets of parallelly arranged strands observed in the H_{II}^C and L_α^C phases (Figure 1), respectively. Importantly, lipid−DNA complexes in the new phase show high transfection efficiency in murine and human cells, with a significant improvement (about 1 order of magnitude) over the control DOTAP complexes observed in mouse embryonic fibroblasts, which are known to be hard to transfect.

Results and Discussion

Lipid Design and Synthesis. Figure 2 shows the structure and synthesis of MVLBG2. The 3,4-dioleyloxybenzoic acid (DOB) hydrophobic moiety[39,60] (underlaid in yellow in Figure 2) provides stable membrane anchoring without side chain crystallization, as well as miscibility with DOPC and DOPE. The headgroup is based on the amino acid ornithine, which is used as an AB$_2$ branching building block. Terminating a core made up of three (1+2) ornithine molecules (underlaid in green in Figure 2) with carboxyspermine[61,62] as end groups (underlaid in red in Figure 2) yields eight primary and eight secondary amino groups in the headgroup. An ethylendiamine linker (underlaid in blue in Figure 2) connects headgroup and DOB.

(53) Dewa, T.; Ieda, Y.; Morita, K.; Wang, L.; MacDonald, R. C.; Iida, K.; Yamashita, K.; Oku, N.; Nango, M. *Bioconjugate Chem.* **2004**, *15*, 824−830.
(54) Sugiyama, M.; Matsuura, M.; Takeuchi, Y.; Kosaka, J.; Nango, M.; Oku, N. *Biochim. Biophys. Acta* **2004**, *1660*, 24−30.
(55) Usol'tseva, N.; Bykova, V.; Smirnova, A.; Grusdev, M.; Lattermann, G.; Facher, A. *Mol. Cryst. Liquid Cryst.* **2004**, *409*, 29−42.
(56) Grohn, F.; Bauer, B. J.; Amis, E. J. *Macromolecules* **2001**, *34*, 6701−6707.
(57) Schenning, A. P. H. J.; Elissenroman, C.; Weener, J. W.; Baars, M. W. P. L.; Vandergaast, S. J.; Meijer, E. W. *J. Am. Chem. Soc.* **1998**, *120*, 8199−8208.
(58) Cooper, R. G.; Etheridge, C. J.; Stewart, L.; Marshall, J.; Rudginsky, S.; Cheng, S. H.; Miller, A. D. *Chem. Eur. J.* **1998**, *4*, 137−151.
(59) Behr, J.-P.; Demeneix, B.; Leffler, J.-P.; Perez-Mutul J. *Proc. Natl. Acad. Sci. U.S.A.* **1989**, *86*, 6982−6986.

(60) Schulze, U.; Schmidt, H.-W.; Safinya, C. R. *Bioconjugate Chem.* **1999**, *10*, 548−552.
(61) Behr, J.-P. *J. Chem. Soc., Chem. Commun.* **1989**, 101−103.
(62) Huber, M.; Pelletier, J. G.; Torossian, K.; Dionne, P.; Gamache, I.; Charest-Gaudreault, R.; Audette, M.; Poulin, R. *J. Biol. Chem.* **1996**, *271*, 27556−27563.
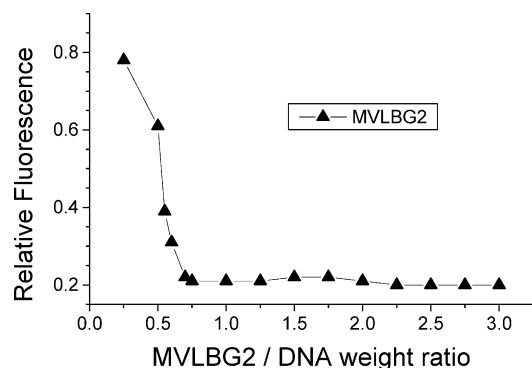
Figure 3. Data from an ethidium bromide (EtBr) displacement assay, used to measure the charge of MVLBG2 in complexes with DNA. Intercalated ethidium bromide is expelled from DNA upon complex formation with cationic lipids, resulting in a reduction in fluorescence intensity due to self-quenching of EtBr in solution. The fluorescence intensity is normalized to that of DNA with EtBr and no lipid. The lines serve as a guide to the eye.

Figure 4. Optical microscopy images of DNA complexes containing (A) 10 mol % and (B) 25 mol % MVLBG2. Complexes were imaged in water using DIC (left), DNA fluorescence (middle), and lipid fluorescence (right) modes. The scale bars correspond to 2 μm. The observation of colocalization of DNA and lipid in the micrometer-scale particles provides direct evidence of the existence of a complex phase at both compositions.

The synthesis of the dendritic headgroup is similar to that of multiple antigenic peptides (MAPs)[63,64] and poly(ethylene glycol) dendritic oligolysine block copolymers.[65] Ornithine methyl ester was first coupled with two (2.2) equivalents of Boc-protected ornithine. After deprotection of the amino groups, a similar coupling was performed using Boc-protected carboxy-spermine.[61,62] Aminolysis of the methyl ester with an excess of ethylenediamine yielded the amine-functionalized spacer-headgroup building block **3**. After coupling with DOB,[60,39] the resulting Boc-protected lipid was purified by flash chromatography and deprotected with TFA. This synthetic route has been carried out on a gram scale and allows facile variation of the spacer length and the headgroup charge by employing other diamines and multivalent headgroup building blocks, respectively.

Ethidium Bromide Displacement Assay. To determine the number of charges per headgroup effective in DNA complexation, we used an ethidium bromide (EtBr) displacement assay.[40,66–68] Increasing amounts of lipid were added to a constant amount of DNA and EtBr, recording the resulting fluorescence and normalizing it to the fluorescence without added lipid. Complex formation of DNA with lipids expels intercalated EtBr, reducing its fluorescence since EtBr self-quenches in solution. As shown in Figure 3, the observed fluorescence drops steeply with increasing amount of added lipid and then levels off to a saturation value. The isoelectric point is obtained from analysis of these data,[40,69,70] yielding the lipid headgroup charge as $Z_{exp} = 15.9 \pm 1.0$. Thus, the headgroup is essentially fully protonated in the complexes.

Optical Microscopy. DNA complexes of MVLBG2 were imaged directly using differential interference contrast (DIC) and fluorescence microscopy. In Figure 4A and B, complexes
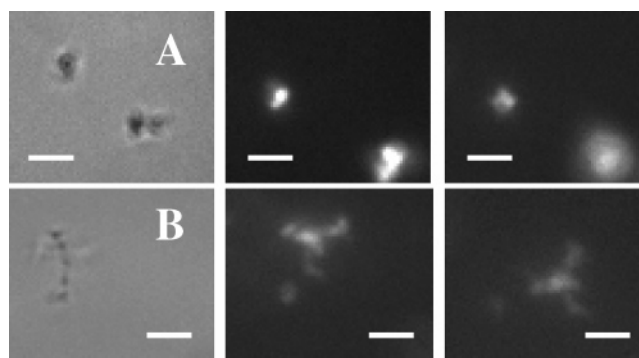
containing 10 and 25 mol % MVLBG2 in the membrane, respectively, are shown. The complexes were prepared in water and doubly labeled with fluorescent DNA and lipid stains. Each complex is imaged in DIC mode (left), DNA fluorescence mode (middle), and lipid fluorescence mode (right). The complex particles, at both lipid compositions, have dimensions on the μm scale, apparently consisting of aggregates of globular submicrometer particles. They are highly mobile, as evident from the drift and rotation of the particles seen in the images. The colocalization observed in the fluorescence imaging modes provides direct evidence of the existence of a phase containing lipid and DNA, a key premise in the analysis of the X-ray scattering data presented below. X-ray diffraction then shows that the compositions imaged here have a very different internal complex structure (see below). In this respect, it is interesting to note that small aggregates of complex particles in the H_{II}^C phase predominantly show branched morphologies[32] similar to that seen in Figure 4B.

X-ray Diffraction. The structure of DNA complexes of MVLBG2 on the nanometer scale was investigated by small-angle X-ray scattering (SAXS). All SAXS experiments were performed in DMEM, the medium used in the transfection experiments. Complexes were formed from mixtures of MVLBG2 and neutral DOPC at a lipid-to-DNA charge ratio of 2.8, placing them in the transfection-relevant regime of cationically charged complexes, where complexes and excess cationic liposomes coexist. While their structure changes significantly with the ratio of neutral to cationic lipid (see below), it is not affected by the lipid-to-DNA charge ratio (ρ_{chg}) above the isoelectric point (data not shown).

As evident from the SAXS pattern shown in Figure 5, complexes containing 10 mol % MVLBG2 form the lamellar phase L_α^C. The peaks (solid arrows) at 0.087, 0.173, and 0.260 Å^{-1} correspond to the q_{001}, q_{002}, and q_{003} reflections from stacks of the lipid bilayers, indicating a layer repeat distance $\delta = 2\pi/q_{001}$ of 72.2 Å. A broader peak, arising from smectic ordering of DNA strands is also visible (q_{DNA}, dashed arrow) and gives their interaxial spacing $d_{DNA} = 2\pi/q_{DNA} = 2\pi/(0.227 \text{ Å}^{-1}) = 27.7$ Å.

At higher mole fractions of MVLBG2 ($\geq 20\%$), the scattering pattern changes significantly. A novel structure, which we describe below, is formed in a narrow range of composition of a few mol % around 25 mol % MVLBG2. At higher contents

(63) Veprek, P.; Jezek, J. *J. Pept. Sci.* **1999**, *5*, 5–23.
(64) Veprek, P.; Jezek, J. *J. Pept. Sci.* **1999**, *5*, 203–220.
(65) Choi, J. S.; Lee, E. J.; Choi, Y. H.; Jeong, Y. J.; Park, J. S. *Bioconjugate Chem.* **1999**, *10*, 62–65.
(66) Gershon, H.; Ghirlando, R.; Guttman, S. B.; Minsky, A. *Biochemistry* **1993**, *32*, 7143–51.
(67) Akao, T.; Fukumoto, A.; Ihara, H.; Ito, A. *FEBS Lett.* **1996**, *391*, 215–218.
(68) Eastman, S. J.; Siegel, C.; Tousignant, J.; Smith, A. E.; Cheng, S. H.; Scheule, R. K. *Biochim. Biophys. Acta Biomembr.* **1997**, *1325*, 41–62.
(69) Ham, Y. W.; Tse, W. C.; Boger, D. L. *Bioorg. Med. Chem. Lett.* **2003**, *13*, 3805–3807.
(70) Boger, D. L.; Fink, B. E.; Brunette, S. R.; Tse, W. C.; Hedrick, M. P. *J. Am. Chem. Soc.* **2001**, *123*, 5878–5891.
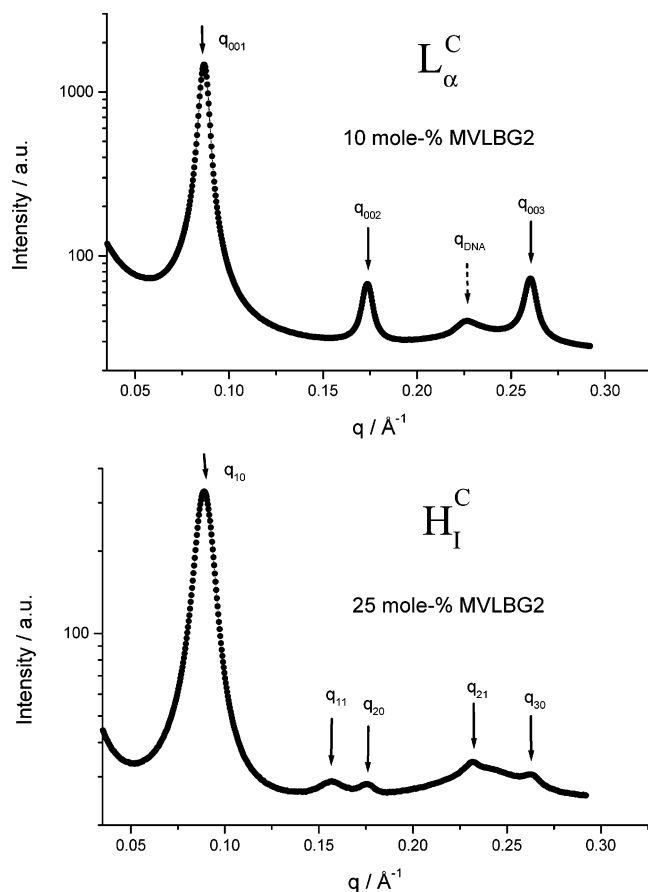
Figure 5. Synchrotron SAXS patterns of DNA complexes of MVLBG2/DOPC mixtures, containing 10 and 25 mol % of the highly charged dendritic lipid. At 25 mol % MVLBG2, the peaks cleanly index to a hexagonal lattice, indicating a change of structure into the new H_I^C phase. Data acquired on SAXS beamline 4-2 at the Stanford Synchrotron Radiation Laboratory.

of MVLBG2, a different phase with lower symmetry is observed.[71] As shown in Figure 5 for 25 mol % MVLBG2, peaks are now found at 0.089, 0.157, 0.177, 0.232, and 0.262 Å^{-1}, corresponding to the q_{10}, q_{11}, q_{20}, q_{21}, and q_{30} reflections of a hexagonal lattice, respectively. Figure 6 shows a schematic of this new hexagonal CL−DNA complex structure, which we term H_I^C. At 20 mol % MVLBG2, complexes in the H_I^C phase are in coexistence with lamellar complexes (data not shown). In the H_I^C phase, tubular lipid micelles are arranged on a hexagonal lattice, with an interaxial distance of $d = 4\pi/(3^{1/2}q_{10}) = 81.5$ Å (Figure 6). The typical thickness of a bilayer formed by lipids with a DOB hydrophobic tail is around 41 Å, which gives a first estimate of the diameter of a lipid tubule formed by MVLBG2. The DNA rods, which have a diameter of 25−30 Å, depending on the extent of hydration, are arranged on a honeycomb lattice in the interstices of the lipid micelle arrangement. It is remarkable that the DNA forms a three-dimensionally contiguous substructure in the H_I^C phase, as opposed to isolated DNA rods and sheets of parallel strands in the H_{II}^C and L_α^C phases (cf. Figure 1), respectively. The remaining interstitial space in the H_I^C structure is filled by the headgroups, water, and counterions which provide local charge neutrality for the complexes at a positive lipid−DNA charge ratio.[72,73] As evident from a comparison of the molecular models
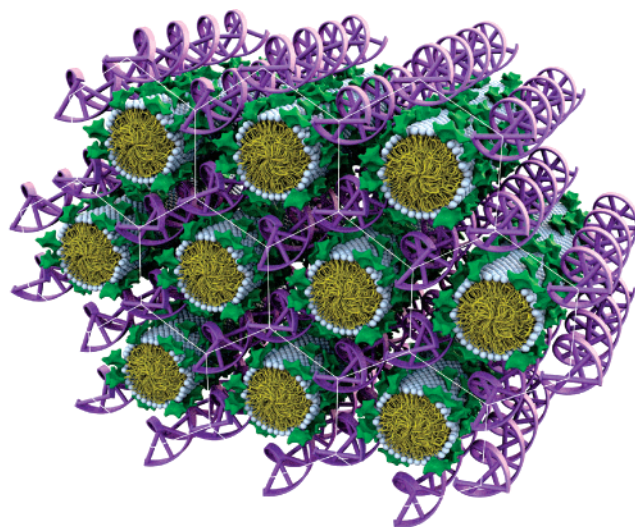

Figure 6. Schematic of the new, H_I^C phase of CL−DNA complexes. The large headgroup of MVLBG2 forces the lipid to assemble into tubular lipid micelles that are arranged on a hexagonal lattice, with an interaxial distance of 81.5 Å (see text). The diameter of the tubular micelles may be estimated to around 41 Å as the typical thickness of a bilayer formed by lipids with DOB hydrophobic tails. The DNA rods, with a diameter of 25−30 Å, are arranged on a honeycomb lattice in the interstices of the lipid micelle arrangement. The remaining interstitial space is filled by the headgroups, water, and counterions. Interestingly, the DNA forms a three-dimensionally contiguous substructure in the H_I^C phase, as opposed to isolated DNA rods and sheets of parallel strands in the H_{II}^C and L_α^C phases (Figure 1), respectively.

of DOTAP (2,3-dioleyloxy-propyl-trimethylammonium chloride)[74] and MVLBG2 shown in Figure 7, the headgroup of MVLBG2 is very large and may fill most of the void space. It is the size of this headgroup that strongly favors a positive curvature of the lipid−water interface and thus leads to the formation of the novel phase.[75] Further corroborating the assignment of the H_I^C structure as opposed to the previously observed H_{II}^C structure is the observation that lipid mixtures containing MVLBG2 are soluble in water over a wide range of composition, indicating the formation of micelles rather than inverted micelles, which have poor water solubility. Structures similar to the H_I^C phase have been proposed for complexes of DNA with cationic detergents, but these structure assignments were less unambiguous since they are based on fewer reflections observed in X-ray scattering experiments.[76−78] In addition, while cationic detergents are highly toxic to cells, and thus their DNA complexes have no potential for medical applications, the DNA complexes of MVLBG2 efficiently transfect cells, as demonstrated below.

Cell Transfection. For transfection studies, we compared DNA complexes of the dendritic lipid MVLBG2 and the commonly used monovalent DOTAP[74] in four different cell lines. Figure 8 shows the effect of varying the lipid to DNA charge ratio ρ_{chg} in mouse fibroblast L-cells. For DOTAP, TE

(71) Evans, H. M.; Ewert, K. K.; Zidovska, A.; Safinya, C. R. Unpublished data.

(72) Bruinsma, R. *Eur. Phys. J. B* **1998**, *4*, 75−88.
(73) Harries, D.; May, S.; Gelbart, W. M.; Ben-Shaul, A. *Biophys. J.* **1998**, *75*, 159−173.
(74) Leventis, R.; Silvius, J. R. *Biochim. Biophys. Acta* **1990**, *1023*, 124−132.
(75) Israelachvili, J. N. *Intermolecular and Surface Forces*; Academic Press: London, 1992.
(76) Ghirlando, R.; Wachtel, E. J.; Arad, T.; Minsky, A. *Biochemistry* **1992**, *31*, 7110−7119.
(77) Mel'nikov, S. M.; Sergeyev, V. G.; Yoshikawa, K.; Takahashi, H.; Hatta, I. *J. Chem. Phys.* **1997**, *107*, 6917−6924.
(78) Zhou, S.; Liang, D.; Burger, C.; Yeh, F.; Chu, B. *Biomacromolecules* **2004**, *5*, 1256−1261.
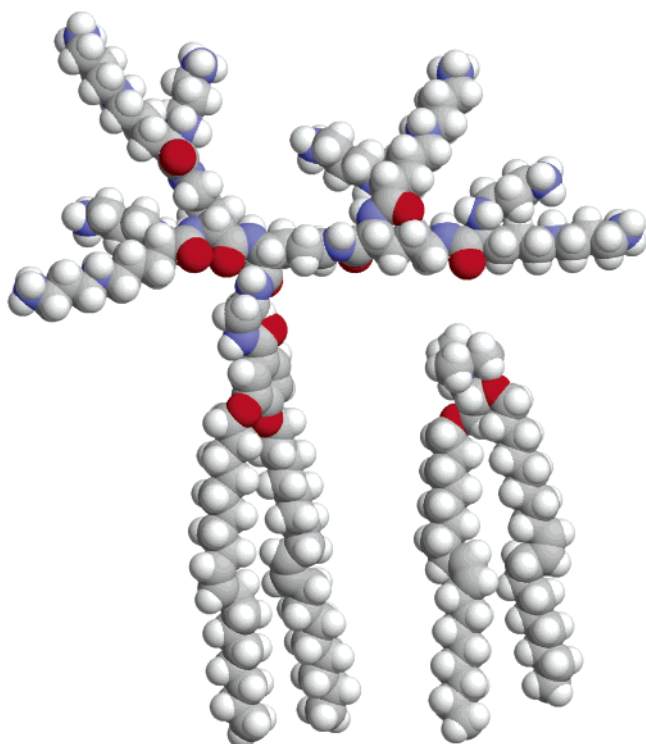
Figure 7. Molecular models of hexadecavalent MVLBG2 (left) and monovalent DOTAP (right).
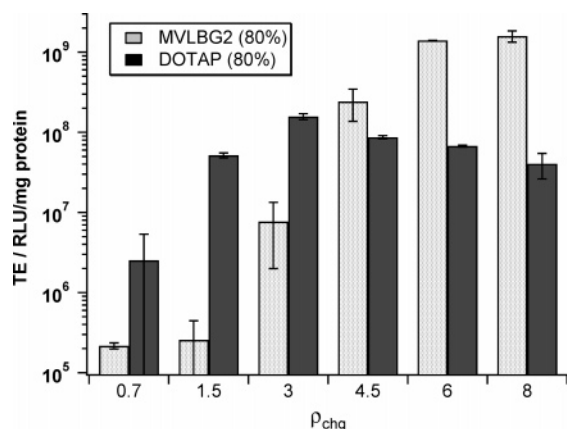

Figure 8. Transfection efficiencies in mouse L-cells for DOTAP/DOPC and MVLBG2/DOPC complexes at 80 mol % cationic lipid, plotted against the lipid/DNA charge ratio ρ_{chg}. While a charge ratio of three is sufficient for optimum performance of DOTAP complexes, the TE of MVLBG2 complexes benefits from higher charge ratios. A typical value of TE for DNA without lipid is 9.6×10^4, corresponding to the starting value of the TE axis.

at all mole fractions of cationic lipid improves with ρ_{chg} up to a saturation value,[79] and the same is observed for MVLBG2. However, the onset of the saturation occurs at a higher charge ratio for the dendritic lipid: $\rho_{chg} = 4.5$ lies in the saturated regime but $\rho_{chg} = 3$ does not, despite marking saturation for DOTAP. Accordingly, all transfection experiments discussed below were performed at $\rho_{chg} = 4.5$ except for those on HeLa cells, where a higher ρ_{chg} of 7 was used to ensure optimum performance of MVLBG2.

Figure 9 shows TE plotted against the mole fraction of cationic lipid for the different cell lines. As a common feature,

we observe that for DOTAP, TE rises exponentially with the fraction of cationic lipid in the membrane from negligible transfection to an optimum at or near 100 mol % DOTAP. This is typical for monovalent lipids in lamellar complexes, which require high membrane charge densities for successful endosomal escape via activated fusion.[40,80] On the other hand, the TE of MVLBG2 complexes reaches a maximum much earlier: 20 mol % (human cell lines) or even 10 mol % (murine cell lines) cationic lipid are sufficient for a TE at or near the highest TE achievable with MVLBG2 complexes. This high level of TE is maintained throughout the remainder of the composition range to 100 mol % MVLBG2, with a slight drop in TE observed for the human cell lines. Comparing the maximum TE for DOTAP and MVLBG2 in the different cell lines, it is evident that the TE achievable with MVLBG2 is as good (293 cells), slightly better (mouse L-cells, HeLa cells), or even significantly better (about 1 order of magnitude for mouse embryonic fibroblast (MEF) cells, 30 mol % MVLBG2 vs 100 mol % DOTAP). The large improvement in MEF cells when using MVLBG2, observed throughout the composition range, is particularly significant since the MEF cells are empirically known to be a "hard to transfect" cell line. This is, however, only one advantage of the multivalent lipid. Another is the ability to add a significant amount of neutral lipid to the vector composition without loss of efficiency, allowing the incorporation of neutral lipids bearing additional (e.g., targeting) functionality into the complex. In addition, since cationic lipid is the component mainly responsible for lipid vector toxicity, the comparatively small number of highly charged cationic lipid molecules required for efficient transfection by MVLBG2 (or more biodegradable analogues) should allow the cationic component of these complexes to be metabolized quickly, resulting in a major advantage for potential applications. Very importantly, the data shows that complexes in the new H_I^C phase and at higher contents of MVLBG2 efficiently transfect murine and human cells, with a TE as high as or higher than that of optimized DOTAP complexes. It is interesting to speculate how the structure of H_I^C complexes may play a role in their transfection mechanism and efficiency. The existence of a continuous DNA substructure likely facilitates release of the DNA cargo, as in principle all DNA is accessible once a part of it is exposed to the inside of the cell. This is in contrast to lamellar complexes, where the enveloping lipid bilayers have to be removed layer by layer to release all encapsulated DNA.

Experimental Section

General Methods. NMR spectroscopy was carried out on a Bruker Avance 200 MHz spectrometer. MALDI-TOF mass spectrometry was performed on a Dynamo spectrometer from Thermal BioAnalysis Ltd. using 2,5-dihydroxybenzoic acid as the matrix and 30 vol.-% water in acetonitrile as the solvent. For thin-layer chromatography, silica covered plastic sheets with fluorescence indicator (Macherey-Nagel) were used. Detection of spots was achieved with UV light and ninhydrin reagent (300 mg in 95 mL of 2-propanol and 5 mL of acetic acid). By addition of methanol to a 4:2:1 (v/v/v) mixture of chloroform, methanol, and 25% ammonia until the mixture became homogeneous, solvent mixture A was obtained. Similarly, solvent mixture B was prepared starting

(79) Slack, N. Ph.D. Dissertation, University of California, Santa Barbara, California, 2000.

(80) Lin, A. J.; Slack, N. L.; George, C. X.; Samuel, C. E.; Safinya, C. R. *Biophys. J.* **2003**, *84*, 3307−3316.
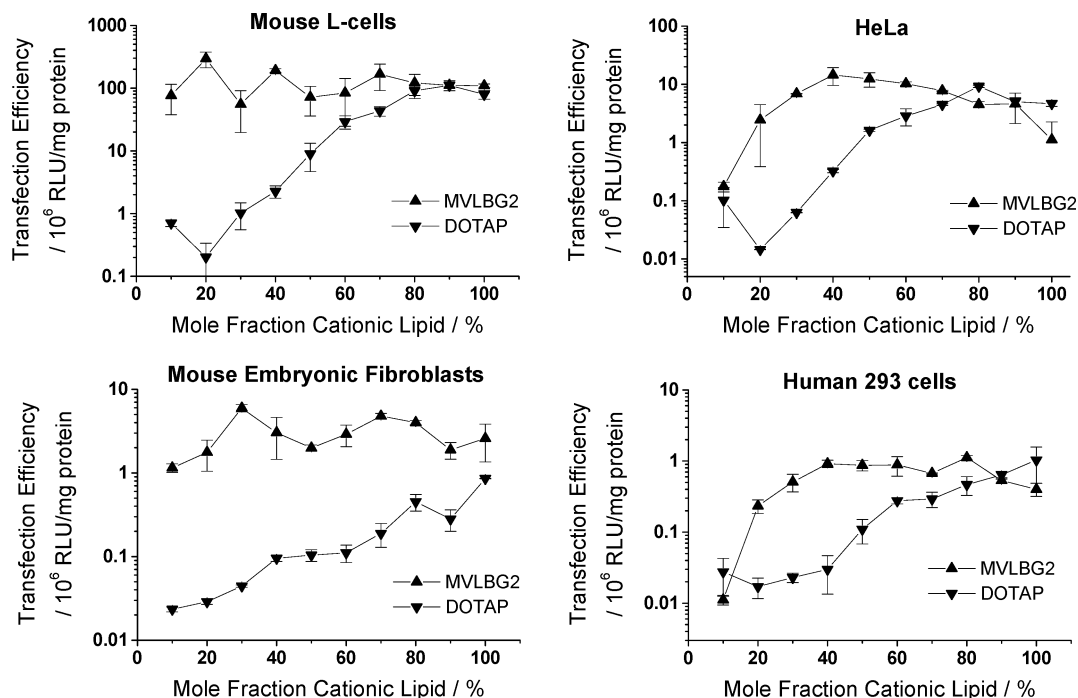
Figure 9. Transfection efficiencies for DOTAP/DOPC and MVLBG2/DOPC complexes in four different cell lines, plotted against the mole fraction of cationic lipid. The data points were obtained at a constant ρ_{chg} (7 for HeLa cells, 4.5 for all others), corresponding to a constant amount of DNA applied to the cells for each data point in a plot.

with a 1:1:1 (v/v/v) mixture of the same solvents. Silica gel from Fisher Scientific with a mesh size of 200–425 was used for flash chromatography.[81]

Lipid Solutions. Stock solutions of MVLBG2 were prepared in chloroform/methanol (9:1, v/v). DOPC and DOTAP were purchased as a solution in chloroform from Avanti Lipids. Lipid solutions were combined at the desired ratio of lipids and dried, first by a stream of nitrogen and subsequently in a vacuum for 8 to 12 h. To the residue, high conductivity (18.2 MΩ) water was added, and the mixture was incubated at 37 °C for at least 12 h to give solutions of a final concentration of 30 mM (DOTAP) or 15 mM (MVLB2) for X-ray samples. For transfection, solutions were prepared at 0.6 mM. Lipid mixtures containing higher mole fractions of DOPC formed opaque suspensions, which were sonicated to clarity and filtered through 0.2 μm filters. The lipid solutions were stored at 4 °C until use.

Ethidium Bromide Replacement Assay. Lipid–DNA complexes were prepared in triplicate by adding a DNA/EtBr mixture to the lipid solution in a 96 well plate. Each well contained 2.4 μg HPCT DNA, 0.28 μg EtBr, and the desired amount of lipid (100% MVLBG2, no DOPC) in a final volume of 250 μL. The emission at 605 nm was measured on a Cary Eclipse fluorescence spectrophotometer, following excitation at 519 nm.

Optical Microscopy. A Nikon Diaphot 300 inverted microscope equipped for epifluorescence and DIC and a SensiCam^{QE} high-speed digital camera were used. For fluorescence microscopy, aqueous lipid stock solutions were prepared at 1 mM with 1 mol % Texas Red-DHPE dye (Molecular Probes). DNA (0.1 mg/mL) was stained using 3.3 mol % (calculated per base pair) YOYO dye (Molecular Probes). Samples were prepared by combining appropriate volumes of lipid and DNA stock solutions to reach a DNA/lipid charge ratio of 2.8 and diluting 2-fold with water. Thirty minutes later, an equal volume of an oxygen scavenging system consisting of 0.5% β-mercaptoethanol, 200 μg/mL glucose oxidase, 35 μg/mL catalase, and 4.5 mg/mL glucose was added to the sample. The complexes were imaged 10 min after the scavenging system was introduced.

Transfection. Wild-type mouse embryonic fibroblast cells were a gift from C. Samuel (UCSB) and originally derived as described (Schreiber, R. D. et al. *Cell* **1998**, *93*, 373–383).[82] The other cell lines were from ATCC (ATCC numbers: mouse fibroblast L-cells: CCL-1; HeLa cells: CCL-2; human 293 cells (kidney-derived fetal epithelial cells): CRL-1573). Cells were cultured at 37 °C in supplemented cell medium (Dulbecco's Modified Eagle's Medium (DMEM) with 1% penicillin–streptomycin and 5% fetal bovine serum, v/v; from Gibco BRL) in an atmosphere containing 5% CO_2 and were reseeded approximately every 72 h to maintain subconfluency. The day before the transfection experiment, cells were seeded in 24-well plates. At the time of transfection, the cells were approximately 70% confluent. Luciferase plasmid DNA (pGL3 Control Vector, Promega) was prepared using a Qiagen Giga Kit (Qiagen). For each well, 0.4 μg of luciferase plasmid DNA was used. Lipid solution (0.6 mM total lipid) was added to the DNA and the mixture was diluted to a final volume of 0.1 mL with nonsupplemented DMEM. The cells were incubated with this solution for 6 h, then rinsed three times with Phosphate Buffered Saline (PBS, Invitrogen) and incubated with supplemented cell media for an additional 24 h. Luciferase gene expression was measured with the Luciferase Assay System (Promega), and light output readings were taken on a Berthold AutoLumat luminometer. Transfection efficiency, measured as relative light units (RLU), was normalized to the weight of total cellular protein determined using Bio-Rad Protein Assay Dye Reagent (Bio-Rad). All experiments were performed at least in duplicate.

Small Angle X-ray Scattering. Lipid solution (see above) was added to 0.2 mg of highly polymerized calf thymus DNA (HPCT, from USB; prepared at 5 mg/mL in water) and mixed with an equal volume of DMEM. Samples were centrifuged for 3 h at 19,000 rpm in a Sorvall SS34 rotor and stored at 4 °C for at least 3 days. Typically, the CL–DNA complexes formed a white precipitate, and these pellets were transferred to 1.5-mm quartz capillaries and flame sealed. Scattering data were collected at beamline 4-2 at the Stanford Synchrotron Radiation Laboratory (SSRL).

(81) Still, W. C.; Kahn, M.; Mitra, A. *J. Org. Chem.* **1978**, *43*, 2923–2925.

(82) Schreiber, R. D. et al. *Cell* **1996**, *84*, 431–442.

Synthesis. Chemicals were from Fisher Scientific and at least of analytical grade unless otherwise indicated. They were used as received. N_α,N_δ-bis(*tert*-Butyl-carbamoyl)ornithine was prepared by a procedure similar to that described in ref 60, which can be found in the Supporting Information.

N_α,N_δ-**bis(2-Cyanoethyl)ornithine (5).** To a solution of 474 mg (11.9 mmol) NaOH in 6 mL of methanol, were added 1.00 g (5.93 mmol) of L-ornithine hydrochloride (Aldrich) and 15 mL of methanol. The mixture was stirred at room temperature, 1.56 mL (1.26 g, 23.7 mmol) of acrylonitrile (Fluka) was added, and stirring was continued for 2 h. The reaction mixture was acidified slightly by the addition of concentrated hydrochloric acid (about 1.5 mL) and filtered immediately. The residue was dried in vacuo to yield 1.4 g (5.66 mmol, 86%) of **5** hydrochloride as colorless microcrystals: $R_f = 0.73$ (solvent mixture A); ^{1}H NMR (D_2O): $\delta = 1.65-2.25$ (m, 4 H, CH_2-CH_2-CH), 2.85–3.1 (m, 4 H), 3.1–3.25 (“t”, 2 H), 3.25–3.7 (“t”, 4 H) (CH_2-N, CH_2-CN), 3.7–3.9 (“t”, 1 H, CH); ^{13}C NMR (D_2O): $\delta = 15.2$, 15.4 (CH_2-CN), 21.8, 26.9 (CH_2-CH_2-CH), 42.7, 43.1, 47.4 (CH_2-N), 62.3 (CH), 118.1 (CN), 172.7 (CO_2H).

N_α,N_δ-**Bis(3-aminopropyl)ornithine (6).** A mixture of 29.8 g (109 mmol) of **5**, 175 mL of 1.4 m NaOH in 95% ethanol, and 6.7 g of a suspension of Raney-nickel (Aldrich) in water was prepared in a Parr hydrogenator flask and agitated for 24 h at room temperature under 60 psi (4 bar) hydrogen pressure. The Raney-nickel was removed by filtration over Celite (diatomaceous earth, acid washed; Sigma), and the solvent was evaporated. The resulting oil was used for the next step without further purification. Pure **6** hydrochloride for analytical purposes was obtained by adding concentrated hydrochloric acid to the reaction solution and collecting and drying the precipitate: ^{1}H NMR (D_2O): $\delta = 1.65-2.25$ (2 m, 8 H, $C-CH_2-C$), 3.0–3.35 (m, 10 H, CH_2-N), 4.12 (t, $^3J = 6.0$ Hz, 1 H, CH); ^{13}C NMR (D_2O): $\delta = 21.8$, 24.1, 24.2, 26.2 ($C-CH_2-C$), 37.0 ($CH_2-NH_3^+$), 44.2, 45.0, 47.2 ($CH_2-NH_2^+$), 59.9 (CH), 170.8 (CO_2H).

N_α,N_δ-**Bis(*tert*-butyl-carbamoyl)-N_α,N_δ-bis(3-[*tert*-butyl-carbamoyl-amino]propyl)ornithine (7).** The raw **6** (assay calculated for 100% yield from the previous step: 108 mmol) was dissolved in water/THF (5:1, v/v). Over the course of 1 h, 100 mL of 4 M NaOH and a solution of 104.2 g (477 mmol) of Boc$_2$O (Novabiochem) in 200 mL of THF were added in four portions with stirring while the reaction mixture was kept at room temperature by cooling with a water bath. Stirring was continued for 6 h, and most of the THF was then evaporated. After addition of 600 mL of diethyl ether and 200 mL of water, the mixture was acidified using half-concentrated hydrochloric acid. The phases were separated, and the aqueous phase was extracted two more times with 200 mL of ether. The combined organic phases were washed twice with water, dried (Na$_2$SO$_4$), and evaporated. The residue was purified in portions of 44 g by flash chromatography on 930 g of silica gel using chloroform/methanol (19:1) as the eluent[83] to yield 26.5 g (41 mmol, 38%) of **7** as a colorless solid: $R_f = 0.72$ (9:1 CHCl$_3$/MeOH); ^{1}H NMR (CDCl$_3$): $\delta = 1.37$, 1.38 (2s, CH_3), 0.8–2.2 (ms, $C-CH_2-C$) (44 H), 2.7–3.9 (ms, 10 H, CH_2-N), 4.26 (bm, 1 H, CH), 5.1–5.5 (b/m, 2 H, NH), 8.58 (b, 1 H, $COOH$); ^{13}C NMR (CDCl$_3$): $\delta = 25.3$, 27.5, 28.7, 29.8 ($C-CH_2-C$), 28.4 ($C(CH_3)_3$), 37.4, 43.8, 44.4, 45.2 (CH_2-N), 59.3 (CH), 79.0, 79.7, 80.8 (CCH_3), 155.5, 156.1 ($O-C(O)-N$), 174.9 (CO_2H).

General Procedure for TBTU-Mediated Coupling (Amine Compound with *n* Amino Groups). To a mixture of 1.1*n* mmol acid component, 1.1*n* mmol *O*-benzotriazol-1-yl-*N,N,N′,N′*-tetramethyluronium tetrafluoroborate (TBTU; Bachem), and 1.1*n* mmol 1-hydroxybenzotriazole (HOBt) hydrate (Peptides International) in dimethylformamide (DMF) (peptide synthesis grade, Applied Biosystems), was added 2*n* mmol *N,N*-diisopropylethylamine (DIEA; Aldrich). After 10 min, a mixture of 1 mmol amine compound (hydrochloride or

hydrotrifluoroacetate form) and *n* mmol DIEA in DMF was added to the resulting solution with stirring. Stirring was continued at room temperature for 2 h, and chloroform and water were added with vigorous stirring after evaporation of most of the DMF.[84] The phases were separated, and after extracting two more times with chloroform, the organic phases were combined and washed twice with 2 M HCl, twice with 2 M NaOH, and once with water. After drying (Na$_2$SO$_4$), the solvents were evaporated.

Methyl (2*S*)-2,5-Di[(1*S*)-1,4-di(*tert*-butyl-carbamoyl-amino)butyl]carboxamidopentanoate (1). As described in the general procedure for TBTU-mediated coupling ($n = 2$), 14.6 g (44.0 mmol) of N_α,N_δ-bis(*tert*-Butyl-carbamoyl)ornithine was reacted with 4.38 g (20 mmol) of ornithine methyl ester dihydrochloride (Bachem) to yield 14.1 g (18.2 mmol, 91%) of **1** as a colorless solid: $R_f = 0.52$ (CHCl$_3$/MeOH, 9:1, 1% AcOH); ^{1}H NMR (CDCl$_3$): $\delta = 0.8-2.1$ (m, $C-CH_2-C$), 1.37 (s, $C(CH_3)_3$), 2.9–3.5 (2 m, 6 H, CH_2-N), 3.65 (s, 3 H, OCH_3), 4.1–4.5 (2 m, 3 H, CH), 4.8–5.1 (bm, 2 H), 5.4–5.8 (2 b, 2 H), 7.22 (b, 1 H), 7.55 (b, 1 H) (all NH); ^{13}C NMR (CDCl$_3$): $\delta = 25.4$, 25.8, 26.1 ($CH_2-CH_2-CH_2$), 28.3, 28.4 ($C(CH_3)_3$), 30.0 (CH_2-CH_2-CH), 38.7, 39.6 (CH_2-NH), 52.2 (OCH_3), 52.1, 53.5, 53.9 (CH), 79.1, 80.0 ($C(CH_3)_3$),156.2 ($O-C(O)-N$), 172.1, 172.9, 173.2 ($C-C(O)$).

Methyl (2*S*)-2,5-Di[(1*S*)-1,4-diaminobutyl]carboxamidopentanoate (8). About 70 mL of TFA (Acros) was saturated with nitrogen, cooled on ice, and added to 10.0 g (12.9 mmol) of **1**. The mixture was evaporated after stirring for 1 h at room temperature, and diethyl ether (300 mL) was added. The ether was decanted, and the solid product was triturated with ether and finally dried in vacuo to yield 4.54 g (12.1 mmol, 94%) of **8** (trifluoroacetate) as a colorless solid: ^{1}H NMR (MeOH-d_4): $\delta = 1.5-2.1$ (m, 12 H, $C-CH_2-C$), 2.9–3.1 (m, 4 H, $CH_2-NH_3^+$), 3.2–3.4 (m, 2 H, CH_2-NH), 3.74 (s, 3 H, OCH_3), 3.92 (“t”, 1 H), 4.04 (“t”, 1 H), 4.50 (“q”, 1 H) (CH); ^{13}C NMR (MeOH-d_4): $\delta = 23.8$, 24.1, 26.5, 29.5 ($C-CH_2-C$), 40.0, 40.1 (CH_2-NH), 53.0, 53.6, 53.9 (CH, OCH_3), 169.9, 170.1, 173.6 ($C(O)$).

Methyl (2*S*)-2,5-Di[(1*S*)-1,4-di[((1*S*)-1,4-di(*tert*-butyl-carbamoyl)-(3-[*tert*-butyl-carbamoyl-amino]propyl)aminobutyl)carboxamido]butylcarboxamido]pentanoate (2). As described in the general procedure for TBTU-mediated coupling ($n = 4$), 5.83 g (9.01 mmol) of **7** was reacted with 1.70 g (2.05 mmol) of **8** to yield 5.15 g (1.78 mmol, 87%) of **2** as a colorless solid: $R_f = 0.53$ (CHCl$_3$/MeOH 9:1, 1% concentrated NH$_4$OH); 0.80 (CHCl$_3$/MeOH 6:1, 1% concentrated NH$_4$OH); For characterization purposes, a small sample was deprotected by adding cold TFA, stirring for 1 h and subsequent evaporation in vacuo: ^{1}H NMR (D_2O): $\delta = 1.2-2.0$ (m, 44 H, $C-CH_2-C$), 2.6–3.2 (m, 52 H, CH_2-N), 3.43 (s, 3 H, OCH_3), 3.55–3.85, 3.90–4.15 (2 m, 7 H, CH), 7.2–7.7, 8.2–8.5 (m, amide-H); ^{13}C NMR (D_2O): $\delta = 21.2$ (2), 21.4 (2), 23.9 (4), 24.0 (4), 24.6, 24.8 (2), 27.1 (4), 28.0, 28.7 (2) ($C-CH_2-C$), 36.7 (8) ($CH_2NH_3^+$), 39.0, 39.4 (2), 43.8 (4), 44.8 (4), 47.0 (4) (CH_2-N), 52.9, 53.1, 54.0, 54.4, 60.0 (2), 60.4(2) (CH, OCH_3), 116.3 (q, $J = 291$ Hz, CF_3), 162.4 (q, $J = 36$ Hz, $CF_3C(O)$), 167.8 (2), 167.6 (2), 172.9, 173.2, 173.9 ($C(O)$).

*N*1-(2-Aminoethyl)-(2*S*)-2,5-di((1*S*)-1,4-di[((1*S*)-1,4-di(*tert*-butyl-carbamoyl)(3-[*tert*-butyl-carbamoyl-amino]propyl)aminobutyl)carboxamido]butylcarboxamido)pentanamide (3). To a solution of 2.00 g (0.69 mmol) of **2** in methanol, was added 927 µL (830 mg, 13.8 mmol) of ethylenediamine in one portion, and the mixture was stirred at room temperature for 10 days. The solvent was evaporated, and water and chloroform were added. After agitation, the phases were separated, and the organic layer was washed two more times with water, dried (Na$_2$SO$_4$), and evaporated. The residue was purified by flash chromatography on 120 g of silica gel using chloroform/methanol (15:1, changed to 6:1 once the product started to elute) as the eluent to yield 1.33 g (0.45 mmol, 66%) of **3** as a colorless solid: $R_f = 0.61$ (CHCl$_3$/MeOH 6:1, 1% concentrated NH$_4$OH); ^{1}H NMR (CDCl$_3$, trace MeOH-

---

(83) This compound elutes faster than estimated by thin-layer chromatography, probably because its retention factor increases with its concentration.

(84) Due to the sensitivity of the methyl ester to hydrolysis, immediate workup of the reaction mixture is mandatory after the addition of water.

d_4): δ = 0.8−2.1 (m), 1.42, 1.44, 1.46 (3 s) (C−**CH₂**−C, C(**CH₃**)₃, 188 H), 2.7−3.5 (m, 50 H, **CH₂**−N), 4.1−4.5 (bm, 7 H, **CH**); ^{13}C NMR (CDCl₃): δ = 25.3, 26.1, 29.9 (C−**CH₂**−C), 28.3 (C(**CH₃**)₃), 37.4, 38.0, 39.1, 40.7, 43.1, 43.7, 44.3, 44.7, 46.4 (**CH₂**−N), 52.4, 55.7, 58.1, 59.0 (**CH**), 78.8, 79.5, 80.7, 80.8 (**C**(CH₃)₃), 155.5, 156.1 (O−**C**(O)−N), 171.8, 172.5 (C−**C**(O)); MALDI-MS: m/z = 2917.3 (M + H$^+$), 2939.1 (M + Na$^+$).

N-1-2-[(1*S*)-1,4-Di((1*S*)-1,4-di[(*tert*-butyl-carbamoyl)(3-[*tert*-butyl-carbamoyl-amino]propyl)amino]butyl)carboxamido]butylcarbox-amido)butylcarboxamido]ethyl-3,4-di[(*Z*)-9-octadecenyloxy]benz-amide (9). A solution of 301 mg (460 μmol) of DOB^{60,39} in dichloromethane was added to a mixture of 148 mg (460 μmol) of TBTU and 71 mg (460 μmol) of HOBt hydrate in DMF. Following the addition of 216 μL (160 mg, 1.24 mmol) of DIEA, the mixture was left to stand for 10 min, and a solution of 1.22 g (418 μmol) of **3** in DMF was added. After standing for 4 h, the solvents were evaporated. Following the addition of chloroform and 5% citric acid and agitation, the phases were separated, and the organic phase was washed one more time with 5% citric acid, twice with 10% NaHCO₃, and once with water. After drying (Na₂SO₄), the solvent was evaporated, and the residue was purified by flash chromatography on 100 g of silica gel using chloroform/methanol (25:1) as the eluent^{83} to yield 1.29 g (364 μmol, 87%) of **9** as a colorless solid: R_f = 0.28 (CHCl₃/MeOH 19:1); ^{1}H NMR (CDCl₃): δ = 0.76 CH₂−**CH₃**), 0.9−2.3 (several m, lg. peaks at 1.16, 1.21, 1.31, 1.33, 244 H, C−**CH₂**−C, C(**CH₃**)₃), 2.7−3.7 (m, 50 H, N−**CH₂**), 3.89 (("t", 4 H, O−**CH₂**), 4.0−4.5 (bm, 7 H, **CH**), 4.7−5.7 (m, 12 H, **=CH**−, **NH**), 6.5−7.8 (several m and b, 11 H), **H**$_{ar}$, **NH**); ^{13}C NMR (CDCl₃): δ = 13.9 (**CH₃**), 22.5 (**CH₂**−CH₃), 25.3 (very b), 25.9, 27.0, 29.1, 29.3, 29.6, 31.7 (C−**CH₂**−C), 28.3 (C(**CH₃**)₃), 37.5, 38.0, 39.4, 39.9, 42.3, 43.7, 44.3, 46.4 (**CH₂**−N), 52.1, 54.7, 58.6, 59.3 (very b, **CH**), 68.9, 69.1 (**CH₂**−O), 78.7, 79.5, 80.6, 80.8 (**C**(CH₃)₃), 112.1, 112.9, 120.0 (**C**$_{ar}$H), 126.6 (**C**$_{ar}$−C(O)N), 129.6, 129.7 (**=CH**−CH₂), 148.6, 151.7 (**C**$_{ar}$−O), 155.4, 156.0 (b, O−**C**(O)−N), 167.5, 171.4, 172.8, 172.5 (C−**C**(O)).

N-1-2-[((1*S*)-1,4-Di[(1*S*)-1,4-di((1*S*)-1,4-di[(3-aminopropyl)amino]-butylcarboxamido)butyl]carboxamidobutyl)carboxamido]ethyl-3,4-di[(*Z*)-9-octadecenyloxy]benzamide (MVLBG2, 4). 9 (1.30 g (366 mmol)) was dissolved in 10 mL of 95% TFA (5% water), which had been saturated with nitrogen and cooled on ice. The mixture was left to stand at room temperature for 25 min with occasional swirling, and most of the TFA was then evaporated in vacuo. A mixture of diethyl ether/pentane (1:1, 30 mL/g protected lipid) was added with stirring, and the precipitate was isolated by decanting. This was repeated twice, and the precipitate was dried in vacuo to yield 1.31 g (348 μmol, 95%) of **MVLBG2** as a colorless solid: R_f = 0.07 (solvent mixture B); ^{1}H NMR (MeOH-d_4): δ = 0.88 ("t", **CH₃**), 0.8−2.4 (several m, lg. peaks at 1.29, 1.35, C−**CH₂**−C) (106 H), 2.85−3.65 (m, 50 H, N−**CH₂**), 3.8−4.2 (m, 8 H, O−**CH₂**, **CH**), 4.2−4.6 (m, 3 H, **CH**), 5.2−5.45 (m, 4 H, **=CH**−), 6.98 (d, ^3J = 8.6 Hz, 1 H, **H**$_{ar}$ *m*-C(O)), 7.4−7.55 (m, 2 H, **H**$_{ar}$), 8.1−9.2 (m, **NH**); ^{13}C NMR (MeOH-d_4): δ = 14.6 (**CH₃**), 22.5, 22.9, 23.8, 25.4, 25.5, 26.6, 27.5, 28.3, 28.5, 30.5, 30.6, 30.7, 30.8, 30.95, 31.01, 33.2 (C−**CH₂**−C), 38.0, 38.5, 40.1, 40.4, 45.0, 45.9, 46.0, 48.2 (**CH₂**−N), 54.6, 55.2, 61.0, 61.4 (**CH**), 70.3, 70.8 (**CH₂**−O), 113.9, 114.3, 122.5 (**C**$_{ar}$H), 118.2 (q, J = 293 Hz, **CF**), 127.6 (**C**$_{ar}$−C(O)N), 130.9, 131.0 (**=CH**−CH₂), 150.2, 154.0 (**C**$_{ar}$−O), 163.3 (q, J = 35 Hz, TFA **C**(O)), 168.6, 168.7, 168.9, 169.0, 170.2, 173.7, 173.8, 174.4 (**C**(O)); MALDI-MS: m/z = 1951.0 (M + H$^+$).

Supporting Information Available: Complete ref 82; full experimental details for the synthesis of N_α,N_δ-bis(*tert*-butyl-carbamoyl)ornithine and corresponding characterization data. This material is available free of charge via the Internet at http://pubs.acs.org.

JA055907H